Available online at www.sciencedirect.com
ScienceDirect
Plant Science 173 (2007) 567–576
PLANT SCIENCE
www.elsevier.com/locate/plantsci

The effects of increased expression of an *Arabidopsis* HD-ZIP gene on leaf morphogenesis and anther dehiscence☆

Qian-Jin Li [a,b], Bing Xu [a,b], Xiao-Ya Chen [a], Ling-Jian Wang [a,*]

[a] *National Key Laboratory of Plant Molecular Genetics, Institute of Plant Physiology and Ecology, Shanghai Institutes for Biological Sciences, Chinese Academy of Sciences, Shanghai 200032, China*
[b] *Graduate School of Chinese Academy of Sciences, Shanghai 200032, China*

Received 28 June 2007; received in revised form 24 August 2007; accepted 28 August 2007
Available online 6 September 2007

Abstract

Of the homeodomain protein superfamily homeodomain-leucine zipper (HD-ZIP) proteins form a plant-specific subfamily. A number of HD-ZIP transcription factors have been reported to play important roles in various aspects of plant growth and development, however, functions of most members remain unknown. Here, we report the characterization of an *Arabidopsis* semidominant mutant, *upcurved leaf1* (*ucl1*). Besides having upcurved leaves, the homozygous mutant plants are male sterile due to anther non-dehiscence. Molecular and genetic analysis indicated that the phenotypes of *ucl1* were resulted from increased expression of *At2g32370*, which encodes a member of class IV HD-ZIP protein, HDG3. We isolated the full-length cDNA of *HDG3* and found a splicing site different from the annotated information. RT-PCR analysis indicated that *HDG3* is specifically expressed in flowers and the promoter-GUS analysis revealed that it is only expressed in anthers. In homozygous *ucl1* anthers, the expression levels of three positive regulators of anther dehiscence, *MYB26*, *NST1* and *NST2* were down-regulated. Taken together, our data demonstrate that *HDG3* plays a negative role in role in regulation of anther dehiscence.

Keywords: HD-ZIP; Anther dehiscence; T-DNA insertion

1. Introduction

Homeodomain proteins, an important group of transcription factors in plants and animals, are characterized by a conserved domain which is encoded by a 180-bp consensus DNA sequence called homeobox [1,2]. Plant homeobox genes form a large family encoding transcription factors that play important roles in various growth and developmental processes, including meristem activity, leaf adaxial–abaxial axis establishment, vascular development, and so on [3,4]. Homeodomain-leucine zipper (HD-ZIP) proteins, characterized by a homeodomain followed by a leucine zipper, make up of a group of plant-specific transcription factors [5].

The *Arabidopsis thaliana* genome probably encodes 89 homeodomain proteins, of them 47 members belong to the HD-ZIP subfamily [6], which have been divided into four classes [7]. The *Arabidopsis* class IV HD-ZIP contains 16 members [8,9]; the first identified and well-characterized gene is *GLABRA2* (*GL2*), which plays a crucial role in both root non-hair cell formation and epidermal trichome development [10–12]. Recent studies indicated that *GL2* is also involved in the control of seed oil accumulation [13]. Other identified class IV HD-ZIP genes include *FWA*, *ANTHOCYANINLESS2* (*ANL2*), *ARABIDOPSIS THALIANA MERISTEM LAYER1* (*ATML1*), and *PROTODERMAL FACTOR2* (*PDF2*). The *FWA* gene was identified from a dominant late-flowering mutant whose *FWA* is ectopically expressed because of epigenetic hypomethylation in the 5′-region of the gene [14,15]. *ANL2* is involved in anthocyanin accumulation and in root development [16]. *ATML1* and *PDF2*, a pair of homeobox genes sharing a very high similarity, are mainly expressed in the outermost cell layer (L1) of shoot apical meristem [8,17]. The single knockout mutant of either *ATML1* or *PDF2* exhibits normal phenotype with respect to growth and morphology, whereas the double mutant displays severe defects in shoot epidermal cell differentiation, suggesting that

☆ The nucleotide sequence reported in this paper has been submitted to the EMBL/GenBank Database under the accession number EF988635.

* Corresponding author. Tel.: +86 21 54924034; fax: +86 21 54924015.
E-mail address: ljwang@sibs.ac.cn (L.-J. Wang).

0168-9452/$ – see front matter © 2007 Elsevier Ireland Ltd. All rights reserved.
doi:10.1016/j.plantsci.2007.08.011

PDF2 and *ATML1* are functionally redundant and are required for maintaining the identity of L1 cells [8]. The remaining genes of the class IV HD-ZIP were named *HOMEODOMAIN GLABROUS1* (*HDG1*) through *HDG12*, in which *HDG6* is identical to *FWA* [9,18]. Functions of these genes, except *HDG6*/*FWA*, have not been elucidated by using loss-of-function mutants, possibly because of functional redundancy among these genes. Alternatively, ectopic or high expression of these genes may cause developmental abnormalities, thus providing new insight into their functions. Here, we report that elevated expression of one of the HD-ZIP IV family genes, *HDG3* (*At2g32370*), gives rise to leaf morphological change and male sterility. Promoter activity and gene expression pattern suggest that *HDG3* is involved in anther dehiscence.

2. Materials and methods

2.1. Plant materials and growth conditions

Plants of *A. thaliana* ecotype Columbia-0 (Col-0) were grown in greenhouse at 20 °C in long day condition (16 h of light). *ucl1* mutant was isolated from a T1 generation transformed with pBI121 vector. The homozygous T-DNA insertion allele *hdg3-1* (SALK_033462c) was obtained from the Arabidopsis Biological Resource Center (Ohio State University, Columbus, OH).

2.2. Identification of T-DNA insertion site and Southern blot analysis

Arabidopsis genomic DNA was isolated and then subjected to TAIL-PCR as described [19]. The PCR products were sequenced, and the T-DNA insertion site was identified by aligning the sequence with *A. thaliana* genome. Three primers (T-DNA left border primer: LBa1, 5′-TGGTTCACG-TAGTGGGCCATCG-3′; genome primers: LP, 5′-AGGCTTT-TATTCAGGGGGCTTAC-3′ and RP, 5′-TTTTCAACTGT-TCCCAATGTTTC-3′) were used to identify heterozygous and homozygous mutants.

After digestion with *Eco*RI or *XbaI*, genomic DNAs (20 μg in each lane) were separated on agarose gel (1.2%) and transferred to a Hybond-N^+ filter membrane (Amersham, Buckinghamshire, UK). The fragment of *NPTII* amplified from pBI121 was used as a probe, which was labeled with ^{32}P-dCTP using a Random Primer DNA Labeling kit (TaKaRa, Dalian, China). Membranes were hybridized and washed according to the manufacturer's manual (TOYOBO, Osaka, Japan).

2.3. RNA analysis

Total RNAs were isolated using TRIzol reagent according to the manufacturer's manual (Invitrogen, Carlsbad, CA). Total RNAs of 1 μg were reverse transcribed in a 20-μL reaction using the RNA PCR (AMV) kit (TaKaRa, Dalian, China), and the diluted products were applied for a 20-μL PCR amplification reaction using gene-specific primers. Quantitative real-time PCR analysis was performed by using Real-Time PCR Core Kit (TaKaRa, Dalian, China) and EvaGreen™ (Biotium) as the dye. *UBQ10* was used as the internal control.

The 5′ UTR sequence of *HDG3* was obtained by RACE-PCR with a GeneRacer™ Kit (Invitrogen, Carlsbad, CA). The specific primers used in RACE-PCR were SP1 (5′-GCCTCCA-CACTTAGGGCATAAGG-3′), and SP2 (5′-CCTTTGTTTGT-CATCTGGGTG-3′).

For RNA gel blot analysis, total RNAs (20 μg in each lane) were separated on a 1.2% denaturing gel and transferred to a Hybond-N^+ filter membrane. The probes were randomly labeled with ^{32}P-dCTP using fragments of *MYB26* and *UBQ10* amplified with the same primers used for RT-PCR.

2.4. Vector construction and plant transformation

A ~1.0 kb fragment upstream of transcription start site of *HDG3* (*At2g32370*) was amplified and inserted into pBI101 and pCAMBIA1300 to generate 101-Pro_{HDG3} and 1300-Pro_{HDG3}, respectively. Then the genomic sequence of *HDG3* was amplified from *ucl1* and cloned into the above vectors to generate 101-Pro_{HDG3}:*HDG3* and 1300-Pro_{HDG3}:*HDG3*, respectively. The vector 101-Pro_{HDG3} and 1300-Pro_{HDG3} were also used to generate 101-Pro_{HDG3}:*GUS* and 1300-Pro_{HDG3}:*GUS* for promoter activity analysis. For RNAi analysis, a 505-bp fragment containing 3′ UTR amplified with primers containing additional appropriate enzymatic recognized sequences (5′-CCTTCCAAATGCTGGTTGAGT-3′ and 5′-TCAACTGAAACAACGAAAGGT-3′). Two copies of this fragment were placed inversely and complementally and spaced out by a 120-nucleotide intron of *Arabidopsis RTM1* gene [20,21]. The fused fragment was inserted into a modified pCAMBIA1300 containing a CaMV 35S promoter and a NOS terminator to generate a double-strands RNA vector, Pro_{35S}:*dsHDG3*. A *GFP* from pCAMBIA1302 fused to 3′ end of *HDG3* was placed in pCAMBIA1300 under the control of a CaMV 35S promoter.

The vectors were introduced into *Agrobacterium tumefaciens* strain GV3101, and the resultant Agrobacteria were infiltrated into *Arabidopsis* by the floral dip method [22].

2.5. Microscopy

Wild-type and mutant plant tissues were observed by scanning electron microscopy as previously described [23]. For histological sections, samples were embedded in Epon812 resin, and transverse sections were made at 2 μm and stained by toluidine blue, and sections were examined microscopically (BX51; Olympus, Tokyo, Japan) and photographed.

Confocal images were obtained with an LSM510 laser scanning confocal microscope (Zeiss, Jena, Germany), with argon laser excitation at 488 nm and a 505–550 nm emission filter set for GFP fluorescence observation.

3. Results

3.1. Isolation and morphological characterization of ucl1 mutant

An *upcurved leaf1* (*ucl1*) mutant was isolated for its distinct phenotype from a T1 population transformed with pBI121. The mutant plant grew slowly and was smaller than the wild-type, and the leaves were upcurved (Fig. 1). The plants of T2 generation segregated into three different phenotypes, namely severe, intermediate, and wild-type-like (Fig. 1A–C).

In addition to smaller stature and strongly upcurved leaves, the severe-phenotyped plants were sterile and developed only short and empty siliques (Figs. 1C and 2A). When pollinated with wild-type pollen, the plants produced normal siliques containing seeds, indicating that plants were male sterile and the female fertility was not affected. Observation with a dissecting microscope revealed that pollen grains were absent from the surface of anthers of the sterile *ucl1* plants (Fig. 2B and C). Scanning electron micrographs showed that the anthers of the sterile plants failed to dehiscence (Fig. 2E and G), whereas wild-type anthers at the same stage opened and the pollen grains were visible (Fig. 2D and F). However, pollen grains could be seen in the locules of the non-dehiscent *ucl1* anthers by transverse section (Fig. 2I). When wild-type plants were pollinated with the pollen grains collected from the *ucl1* anthers opened mechanically, seed-containing siliques were obtained. These observations indicate that, in the sterile *ucl1* mutant, pollen development was unaffected.

After pollinating the homozygous *ucl1* plants with wild-type pollen grains, the F1 progenies all showed the *ucl1* mutant phenotype, and the F2 plants also segregated into three groups on the basis of phenotypes, similar to the T2 progenies of initial mutant. In the F2 population of 190 plants examined, 53 plants showed a severe phenotype, 90 showed an intermediate phenotype, and 47 appeared normal, which fitted the ratio of 1:2:1 ($P > 0.05$). The phenotype of upcurved leaf was co-segregated with kanamycin resistance. Southern blot analysis showed that there was a single copy of T-DNA in the *ucl1* mutant (Fig. 3A). These results suggest that the initial *ucl1* mutant was heterozygous with a semidominant mutation in a single nuclear gene.

To find out the cause of mutant phenotype, we performed TAIL-PCR to locate the T-DNA insertion site. We found that the T-DNA was inserted in chromosome 2 within the intergenic region between *At2g32360* and *At2g32370*. Further sequence analysis showed that the insertion site was located 977 bp upstream of the start codon of *At2g32360*, which encodes an ubiquitin family protein, and 3884 bp upstream of the start codon of *At2g32370* (Fig. 3B), which encodes a HD-ZIP protein that has been designated as *HOMEODOMAIN GLABROUS3* (*HDG3*) [9].

According to the insertion site of T-DNA, we assumed that the abnormal development of *ucl1* plants could be caused by changed expression of either *At2g32360* or *HDG3* (*At2g32370*), or both. We then employed RT-PCR to investigate the expression levels of both genes in wild-type and the mutant plants. The expression level of *HDG3* was evidently increased in mutant plants, whereas the expression level of *At2g32360* was not altered (Fig. 3E). This result suggests that the phenotypic change of *ucl1* plants was caused by an increased expression of *HDG3*.

In order to confirm that the initial *ucl1* mutant is a semidominant mutant, we performed PCR to investigate the T-DNA insertion instance in the severe and intermediate mutant using primer of T-DNA left border and the primers corresponding to the genomic region flanking the insertion site. As expected, the T-DNA insertion was heterozygous in intermediate plants and homozygous in severe plants (data not shown). The semidominant mutation was also validated by quantitative real-time PCR analysis of the expression level in leaves, which showed that the *HDG3* transcript level in

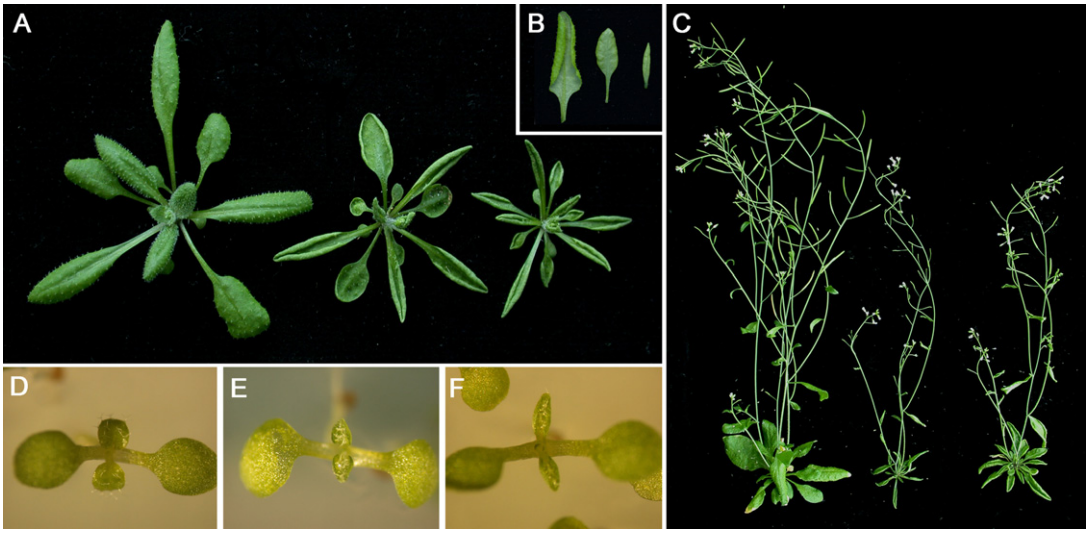

Fig. 1. Morphological comparison of wild-type and *ucl1* mutant plants. (A) The 20-day-old wild-type (left), intermediate *ucl1* (middle) and severe *ucl1* (right) plants grown on soil in greenhouse. (B) The abaxial leaf of 20-day-old plants shown on (A). (C) The 50-day-old wild-type (left), severe *ucl1* (middle) and intermediate *uc1* (right) plants grown on soil in greenhouse. (D–F) The 7-day-old seedling of wild-type (D), intermediate *ucl1* (E) and severe *ucl1* (F) plants grown on 1/2 MS medium.

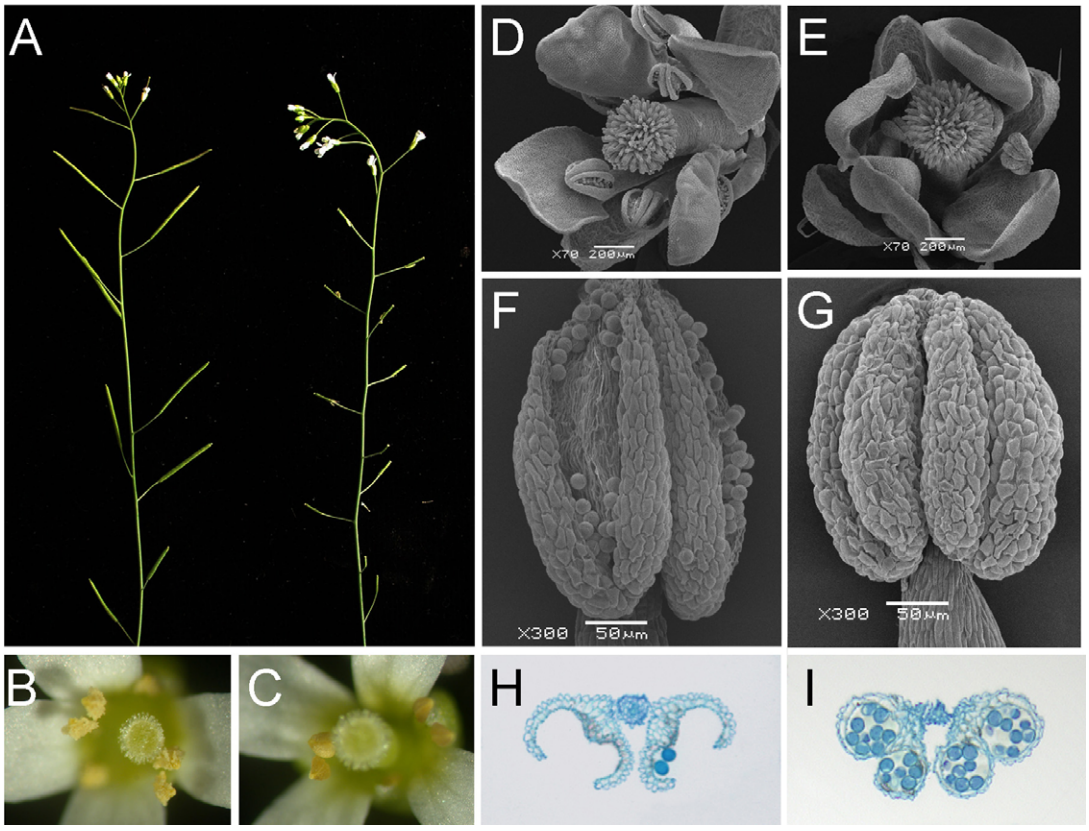

Fig. 2. Comparison of wild-type and *ucl1* homozygous mutant plants. (A) Main branch of 50-day-old wild-type (left) and *ucl1* homozygous (right) plants. (B and C) Flower of wild-type (B) and *ucl1* homozygous (C) plants. (D and E) Scanning electron microscopy image of wild-type (D) and *ucl1* homozygous (E) flower. (F and G) Scanning electron microscopy image of wild-type (F) and *ucl1* homozygous (G) anther of opened flower. (H and I) Toluidine blue-stained cross section of wild-type (H) and *ucl1* homozygous (I) anther of opened flower.

homozygote was about two times as that in heterozygote. The expression of *HDG3* was undetectable in wild-type plant leaves (Fig. 3F).

3.2. Sequence analysis of the HDG3 locus

The genomic sequence of *HDG3* contains 3879 bp, which has been annotated to 10 exons and 9 introns according to the annotation information (http://www.arabidopsis.org). Thus, the annotated cDNA was 2612 bp long, containing a 446-bp 3′ untranslated region (UTR) and an open reading frame coding for a 721-amino acid polypeptide. However, the 5′ UTR was undetermined. To identify the 5′ UTR of *HDG3*, 5′ rapid amplification of cDNA ends (RACE) was performed using *ucl1* total RNA by taking advantage of its overexpression feature. Sequencing of the RACE fragment indicated that the full-length cDNA of *HDG3* contains a 239-bp 5′ UTR. Comparison to the genomic sequence revealed that the transcription start site is 1530 bp upstream of the start codon and in this region there are two introns, which are of 232 bp and 1059 bp long, respectively (Fig. 3D). A putative TATA box was found 31 bp upstream of the transcriptional initiation site. Therefore, the genomic sequence of *HDG3* can be divided into 12 exons and 11 introns based on our RACE result (Fig. 3D). Taken together, in the genome of *ucl1* plant, the T-DNA of pBI121 is inserted at 2354 bp and 3884 bp upstream of the transcription start site and start codon of *HDG3*, respectively, and at the upstream of insertion site, there is a CaMV 35S promoter opposite to the transcription direction of *HDG3* (Fig. 3C).

Based on the annotated 3′ UTR and newly identified 5′ UTR of *HDG3*, we designed a pair of primers and isolated the full-length cDNA through RT-PCR amplification of the transcripts from *ucl1* leaves. Sequencing results of three individual clones revealed that, in comparison with the original annotation, the *HDG3* cDNA contained an additional 12-bp (GTGATCACA-TAA) fragment at the terminal of the ninth exon. In flowers of wild-type plants, the *HDG3* transcripts were faintly detectable (see below). With two-round-PCR amplification, the full-length cDNA of *HDG3* was also obtained from flowers of wild-type plants. Sequence comparison revealed that *HDG3* cDNA from wild-type plants contained the same 5′ UTR and additional 12-bp fragment as that from *ucl1* plants (Fig. 3D). These results indicate that the originally predicted cDNA of *HDG3* was inaccurate, and the splicing site between the ninth exon and the ninth intron should be corrected.

3.3. Confirmation of mutation by transgenic studies

Based on the structural context of T-DNA insertion site (Fig. 3C), we hypothesized that the enhancer of CaMV 35S promoter strengthened the transcription of *HDG3*, which consequently caused the phenotype of *ucl1*. To verify this

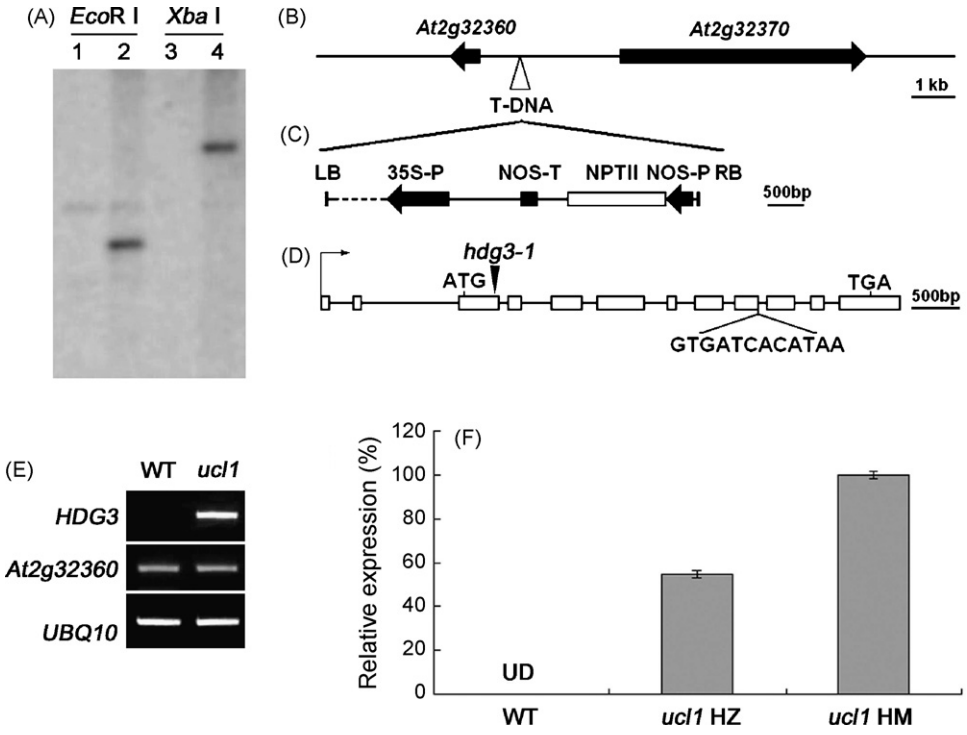

Fig. 3. Identification of T-DNA insertion and cloning of *HDG3*. (A) Southern blot analysis of T-DNA copy number in the *ucl1* mutant. Genomic DNA (20 μg in each lane) of wild-type (lanes 1 and 3) and *ucl1* (lanes 2 and 4) plants was digested with *Eco*RI or *Xba*I and probed against *NPTII* coding region of pBI121. (B) Physical map of the T-DNA insertion site. The arrows indicate the transcription orientation of the open reading frames flanking the integrated T-DNA. (C) Structure of the integrated T-DNA in the *ucl1* genome. (D) Genomic structure of *HDG3*. Arrow indicates transcription start site. ATG and TAA indicate translation start codon and stop codon, respectively. GTGATCACATAA at the terminal of the ninth exon indicates the additional 12-bp fragment in the full-length cDNA of *HDG3* compared with the annotation information. Arrowhead indicates the T-DNA insertion site of *hdg3-1*, a loss-of-function mutant of *HDG3*. (E) RT-PCR analysis of *HDG3* (*At2g3237*0) and *At2g32360* expression in leaves of 25-day-old wild-type (left lane) and *ucl1* plants (right lane). *UBQ10* was used as internal control. (F) Quantitative real-time PCR analysis of *HDG3* expression in leaves of 25-day-old wild-type (WT), *ucl1* heterozygous (*ucl1* HZ) and *ucl1* (*ucl1* HM) homozygous plants. Transcription level in *ucl1* homozygous plants was set as 100%. UD means undetectable. *UBQ10* was used for normalization. Error bars indicate standard error.

hypothesis, we performed two experiments. First, we amplified the genomic sequence of *HDG3* and placed it under the control of its native promoter (about 1000 bp) in the binary vector pCAMBIA1300, which harbored a CaMV 35S promoter in the flank of multiple cloning sites. The resultant construct, named 1300-Pro_{HDG3}:*HDG3*, has structural similarities with the integrated T-DNA in the *ucl1* genome. The *HDG3* gene with its own promoter was also placed in pBI101, which had no CaMV 35S promoter, and the resultant construct was named 101-Pro_{HDG3}:*HDG3*. The two constructs were then introduced into wild-type plants. Among the T1 transformants, a majority of seedlings transformed with 1300-Pro_{HDG3}:*HDG3* showed the *ucl1*-like phenotype (Fig. 4A), whereas the plants transformed with 101-Pro_{HDG3}:*HDG3* did not display obvious phenotypic changes (data not shown). RT-PCR analysis demonstrated that accumulation of *HDG3* transcripts was drastically elevated in *ucl1*-like 1300-Pro_{HDG3}:*HDG3* plants (Fig. 4B). When *HDG3* driven by the CaMV 35S promoter was expressed in wild-type plants, the transgenic plants showed different but partially overlapping phenotypical changes, such as upcurved leaves, slow growth, and aberrant inflorescences, and a high sterile rate (Fig. 4D and E). These observations suggest that the enhancer of CaMV 35S promoter can facilitate the activity of *HDG3* promoter and increase expression level of *HDG3*, causing the abnormal phenotypes observed with *ucl1* mutant.

Second, we introduced a double-stranded RNA construct (Pro_{35S}:*dsHDG3*) containing a 505-bp inverse repeat derived from the 3′ UTR of *HDG3*, driven by the CaMV 35S promoter, into the heterozygous *ucl1* plants. Out of the 88 T1 transgenic lines, 64 exhibited a wild-type-like phenotype and grew normally (Fig. 4F). RT-PCR analysis indicated that the accumulations of *HDG3* mRNA in these phenotype-restored lines were strongly reduced (Fig. 4G). Taken together, these results support that the phenotype of *ucl1* mutant is attributed to elevated expression of *HDG3*.

3.4. Expression pattern of HDG3 and subcellular localization of HDG3 protein

The expression pattern of *HDG3* was examined in various tissues by RT-PCR. For wild-type plants *HDG3* mRNA was detected at a low level only in flowers, and the transcripts were undetectable in leaves, stems, roots and seedlings. Whereas in *ucl1* plants, *HDG3* was expressed in leaves, stems, flowers and seedlings, but not in roots (Fig. 5A). To further dissect the expression pattern, a promoter fragment of ∼1000 bp of *HDG3* was fused to a β-glucuronidase (*GUS*) reporter gene in vector pBI101 to generate 101-Pro_{HDG3}:*GUS*. GUS staining of the transgenic plants showed that the GUS activity was faintly detected only in anthers of the opened flower (Fig. 5B). The

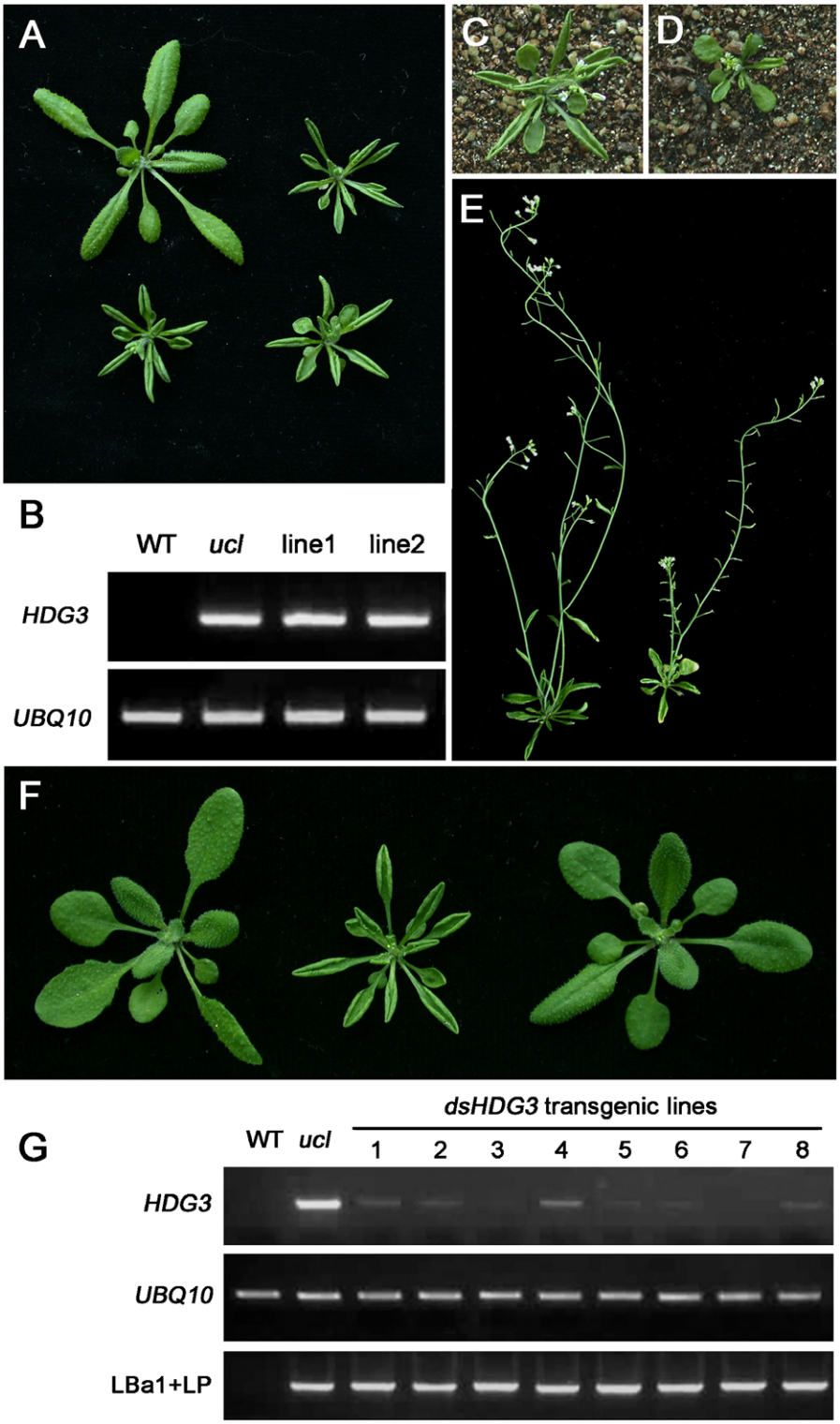

Fig. 4. Comfirmation of mutation by transgenic studies. (A) The 20-day-old wild-type plant (left of top), *ucl1* homozygous plant (right of top) and two individual T1 transformants carrying the construct of 1300-Pro_{HDG3}:*HDG3* (bottom). (B) RT-PCR analysis of *HDG3* expression in plants shown in (A). (C and D) The 28-day-old *ucl1* homozygous plant (C) and T1 transformant carrying the construct of 1300-Pro_{35S}:*HDG3* (D). (E) The 50-day-old *ucl1* homozygous plant (left) and T1 transformant carrying the construct of 1300-Pro_{35S}:*HDG3* (right). (F) 20-day-old wild-type plant (left), *ucl1* heterozygous plant (middle) and one of the phenotype-rescued T1 transformants carrying the construct of Pro_{35S}:*dsHDG3* (right). (G) Molecular analysis of phenotype-rescued transgenic plants transformed with Pro_{35S}:*dsHDG3*. RT-PCR analysis showed decreased accumulation of *HDG3* transcripts in transgenic lines (top panel). PCR analysis showed the background of phenotype-rescued plants was *ucl1* mutant (bottom panel).

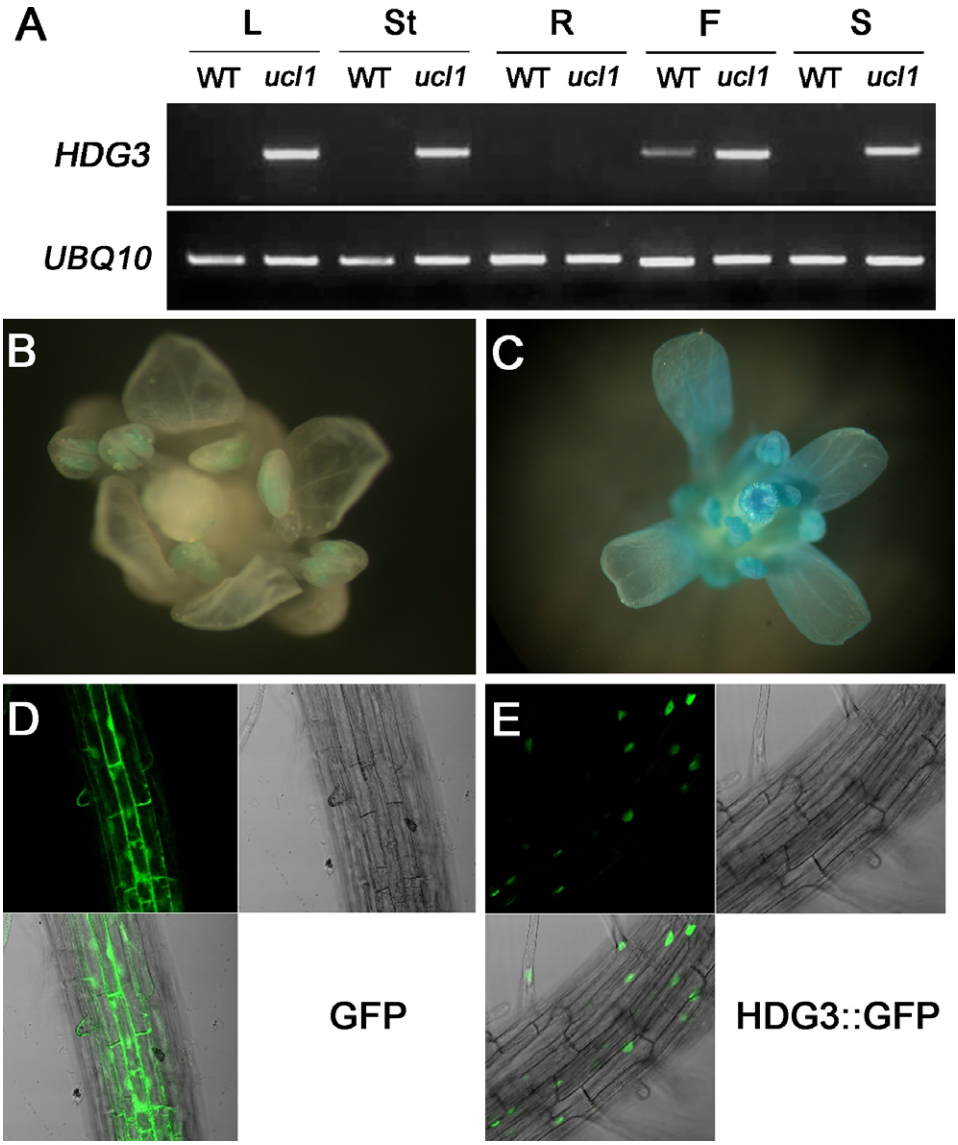

Fig. 5. Expression pattern of *HDG3* and subcellular localization of HDG3. (A) The *HDG3* mRNA accumulation pattern was investigated by RT-PCR with RNA from rosette leaves (L), stems (St), roots (R), flowers (F) and 7-day-old seedlings (S) of wild-type and *ucl1* mutant plants. (B) GUS staining of the transgenic plants carrying 101-Pro_{HDG3}:*GUS*. (C) GUS staining of the transgenic plants carrying 1300-Pro_{HDG3}:*GUS*. (D) Green fluorescence signal in root cells expressing a 35S-driven free GFP. (E) Green fluorescence signal in root cells expressing a 35S-driven HDG3-GFP fusion protein.

same chimeric gene was also cloned into pCAMBIA1300 to generate 1300-Pro_{HDG3}:*GUS*. We found that, in plants transformed with 1300-Pro_{HDG3}:*GUS*, GUS activity was detected in all upground tissues (data not shown) and the activity in flower was expanded to all floral organ (Fig. 5C). In comparison with 101-Pro_{HDG3}:*GUS* plants, the intensity of GUS staining in the anther was stronger in the 1300-Pro_{HDG3}:*GUS* plants (Fig. 5B and C). The extended and stronger expression of 1300-Pro_{HDG3}:*GUS* was likely resulted from the enhancer of the CaMV promoter, which was used to driven the selectable marker gene for hygromycin resistance.

To explore the subcellular localization of HDG3 protein, a green fluorescent protein (GFP) gene was in-frame fused to 3′ end of *HDG3* cDNA driven by a CaMV 35S promoter. Confocal imaging of the roots of 7-day-old transgenic seedlings revealed that HDG3 was a nucleus-localized protein (Fig. 5D and E).

As described above, one of the visible phenotypes of *ucl1* is the poor fertility in the homozygote. To investigate the molecular feature of anther non-dehiscing, we performed RT-PCR to analyze the expression changes of three genes, *MYB26*, *NST1* and *NST2*, which were reported to be positive regulators of anther dehiscence [24–26]. The results showed that expression levels of the three genes in homozygous *ucl1* flowers were down-regulated (Fig. 6A). RNA gel blot analysis also showed a reduced accumulation of *MYB26* mRNA in *ucl1* (Fig. 6B).

In order to investigate the function of *HDG3*, we obtained its T-DNA insertion mutant, *hdg3-1* (SALK_033462) from SALK Institute T-DNA insertion collection. The homozygous *hdg3-1* mutant did not show any visible phenotypic change (data not shown). This is consistent with a previously report by Nakamura et al. that *hdg3-1* and *hdg2-3 hdg3-1*, a double

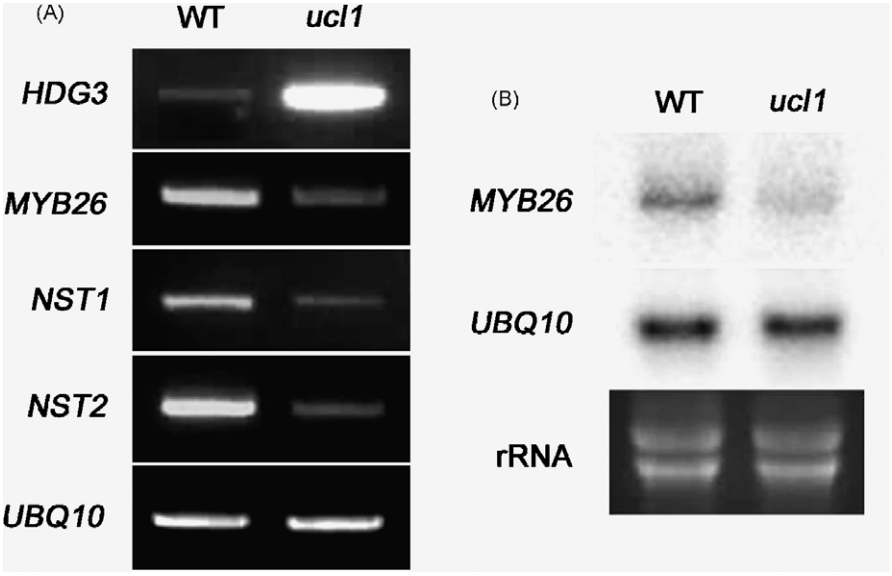

Fig. 6. Expressions of genes involved in anther dehiscence. (A) Expressions of *HDG3*, *MYB26*, *NST1* and *NST2* were investigated by RT-PCR with RNA from flowers of wild-type (left lane) and *ucl1* mutant plants (right lane). (B) Expression of *MYB26* was investigated by RNA gel blot analysis with RNA from the same materials used in (A). *UBQ10* was used as control.

mutant of *HDG3* and its paralogous gene, *HDG2*, appeared normal in growth and development [9]. However, the *hdg3-1 pdf2-1* and *hdg3-1 atml1-1* double mutants showed morphological abnormalities [9]. For functional analysis of *HDG3* and other class IV *HD-ZIP* gene, it will be necessary to construct multiple mutants.

4. Discussion

The class IV HD-ZIP consists of 16 members in *Arabidopsis* genome [8,9]. Except for 5 members, functions of most of the members are still unknown. In this article, we report the isolation of the *ucl1* mutant and molecular characterization of *HDG3*, a member of class IV HD-ZIP genes. Evidences presented here clearly indicate that the *ucl1* phenotype is caused by elevated expression of *HDG3*.

In plants, many genes have functional redundancy, which makes it difficult to discover gene functions through analysis of loss-of-function mutants. Activation tagging with the enhancer from the CaMV 35S promoter provides an effective platform for plant functional genomics research [27]. Activation tagging, which has been developed in several plant species, including *Arabidopsis* [27], rice [28], poplar [29] and barley [30], facilitates functional identification of genes which are functionally overlapping or whose expressions are weak but play an important role in plant growth and development. The *ucl1* mutant, isolated based on its upcurved leaves from a T1 population of transgenic *A. thaliana*. The expression of *HDG3* in *ucl1* is evidently increased in leaves, stems and flowers and seedlings when compared with wild-type plants, in which *HDG3* is only weakly expressed in flowers. In *ucl1* mutant, *HDG3* is not expressed in roots as well as in wild-type plant. Ectopic and constitutive expression of *HDG3* driven by CaMV 35S promoter resulted in severer phenotypes than the *ucl1* mutant (Fig. 4D and E), whereas the transgenic plants carrying the construct of 1300-Pro_{HDG3}:*HDG3* in which *HDG3* was driven by its own promoter showed the *ucl1*-like phenotype (Fig. 4A). These observations suggest that the phenotypes of *ucl1* were resulted from elevated expression of *HDG3*, though ectopic or constitutive expression could not be excluded.

The *ucl1* mutant was generated by genetic transformation with pBI121 vector, which contained a CaMV 35S promoter. In the genome of *ucl1*, the 35S promoter sequence within T-DNA region was reversely inserted upstream of the promoter of *HDG3*. It is likely that the enhancer of 35S promoter is responsible for the elevated expression of *HDG3*, as in the activation tagging screen. This hypothesis was supported by the promoter-GUS analysis. The 1300-Pro_{HDG3}:*GUS* plants showed extended and stronger GUS activity in comparison of the 101-Pro_{HDG3}:*GUS* plants (Fig. 5B and 5C). In the constructs of 1300-Pro_{HDG3}:*GUS*, 35S promoter was used to driven the selectable marker gene for hygromycin resistance, so the enhancer of 35S promoter may boost up the expression of *GUS*. Recently it is reported that the enhancer of 35S promoter used for selectable marker gene of a plant transformation vector can *trans* activate and override the control of the transgene expression [31]. The structure of 1300-Pro_{HDG3}:*HDG3* is similar with that of integrated T-DNA in *ucl1* genome, therefore, it is not unexpected that plants transformed with 1300-Pro_{HDG3}:*HDG3* show similar phenotypes as the *ucl1* mutant.

To facilitate pollination, mature pollen grains must be released from the locules of the anther, which is achieved through a process called anther dehiscence [32]. In *Arabidopsis*, three genes required for anther dehiscence have been identified by genetic studies. *ms35*, the loss-of-function mutant of *MYB26*, and the double mutant of *NST1* and *NST2* completely fail to undergo anther dehiscence due to loss of secondary wall thickening in anther endothecium [24–26]. *MYB26* plays regulatory role in the expression of *NST1* and *NST2* [26]. In the homozygous mutant of *ucl1*, the anthers

failed to dehiscence, resulting in male sterility. In addition, *HDG3* is mainly expressed in anther, consistent with its presumed role in the process of anther dehiscence. In flowers of the *ucl1* homozygous mutant the expressions of *MYB26*, *NST1* and *NST2* were repressed, suggesting that *HDG3* negatively regulates anther dehiscence via controlling the expression of *MYB26*, *NST1* and *NST2* directly or indirectly. To elucidate the regulatory mechanism, the interactions between HDG3 and the promoters of these genes need further investigation. According to the public Arabidopsis microarray databases (http://www.genevestigator.ethz.cn), *HDG3* has a relatively high level of expression in siliques and very low levels in other tissues. Among the tissues we analyzed, the expression of *HDG3* was detected only in flowers at a low level. Previously, Nakamura et al. reported that *HDG3* was weakly expressed in siliques and seedlings [9]. Hence, the possibility that ectopic expression of *HDG3* in *ucl1* led to anther indehiscence cannot be excluded.

Acknowledgements

This work was supported by The National High-tech Research Program of China (2006AA10A109). We thank Xiao-Yan Gao for assistance in scanning electron microscopy and anther section, and Xiao-Shu Gao for assistance in confocal imaging. We are also grateful to Hui-Feng Shen, Bin Luo and Chun-Hong Li for their help and suggestions.

References

[1] W.J. Gehring, M. Affolter, T. Burglin, Homeodomain proteins, Annu. Rev. Biochem. 63 (1994) 487–526.
[2] W.J. Gehring, Y.Q. Qian, M. Billeter, K. Furukubo-Tokunaga, A.F. Schier, D. Resendez-Perez, M. Affolter, G. Otting, K. Wuthrich, Homeodomain-DNA recognition, Cell 78 (1994) 211–223.
[3] M.J. Prigge, D. Otsuga, J.M. Alonso, J.R. Ecker, G.N. Drews, S.E. Clark, Class III homeodomain-leucine zipper gene family members have overlapping, antagonistic, and distinct roles in *Arabidopsis* development, Plant Cell 17 (2005) 61–76.
[4] R.L. Chan, G.M. Gago, C.M. Palena, D.H. Gonzalez, Homeoboxes in plant development, Biochim. Biophys. Acta 1442 (1998) 1–19.
[5] I. Ruberti, G. Sessa, S. Lucchetti, G. Morelli, A novel class of plant proteins containing a homeodomain with a closely linked leucine zipper motif, EMBO J. 10 (1991) 1787–1791.
[6] J.L. Riechmann, J. Heard, G. Martin, L. Reuber, C. Jiang, J. Keddie, L. Adam, O. Pineda, O.J. Ratcliffe, R.R. Samaha, R. Creelman, M. Pilgrim, P. Broun, J.Z. Zhang, D. Ghandehari, B.K. Sherman, G. Yu, *Arabidopsis* transcription factors: genome-wide comparative analysis among eukaryotes, Science 290 (2000) 2105–2110.
[7] G. Sessa, C. Steindler, G. Morelli, I. Ruberti, The *Arabidopsis Athb-8*, *-9* and *-14* genes are members of a small gene family coding for highly related HD-ZIP proteins, Plant Mol. Biol. 38 (1998) 609–622.
[8] M. Abe, H. Katsumata, Y. Komeda, T. Takahashi, Regulation of shoot epidermal cell differentiation by a pair of homeodomain proteins in *Arabidopsis*, Development 130 (2003) 635–643.
[9] M. Nakamura, H. Katsumata, M. Abe, N. Yabe, Y. Komeda, K.T. Yamamoto, T. Takahashi, Characterization of the class IV homeodomain-Leucine Zipper gene family in *Arabidopsis*, Plant Physiol. 141 (2006) 1363–1375.
[10] W.G. Rerie, K.A. Feldmann, M.D. Marks, The *GLABRA2* gene encodes a homeo domain protein required for normal trichome development in *Arabidopsis*, Genes Dev. 8 (1994) 1388–1399.
[11] J.D. Masucci, W.G. Rerie, D.R. Foreman, M. Zhang, M.E. Galway, M.D. Marks, J.W. Schiefelbein, The homeobox gene *GLABRA2* is required for position-dependent cell differentiation in the root epidermis of *Arabidopsis thaliana*, Development 122 (1996) 1253–1260.
[12] Y. Ohashi, A. Oka, R. Rodrigues-Pousada, M. Possenti, I. Ruberti, G. Morelli, T. Aoyama, Modulation of phospholipid signaling by *GLABRA2* in root-hair pattern formation, Science 300 (2003) 1427–1430.
[13] B. Shen, K.W. Sinkevicius, D.A. Selinger, M.C. Tarczynski, The homeobox gene *GLABRA2* affects seed oil content in *Arabidopsis*, Plant Mol. Biol. 60 (2006) 377–387.
[14] W.J. Soppe, S.E. Jacobsen, C. Alonso-Blanco, J.P. Jackson, T. Kakutani, M. Koornneef, A.J. Peeters, The late flowering phenotype of *fwa* mutants is caused by gain-of-function epigenetic alleles of a homeodomain gene, Mol. Cell 6 (2000) 791–802.
[15] Y. Kinoshita, H. Saze, T. Kinoshita, A. Miura, W.J. Soppe, M. Koornneef, T. Kakutani, Control of FWA gene silencing in *Arabidopsis thaliana* by SINE-related direct repeats, Plant J. 49 (2007) 38–45.
[16] H. Kubo, A.J. Peeters, M.G. Aarts, A. Pereira, M. Koornneef, *ANTHOCYANINLESS2*, a homeobox gene affecting anthocyanin distribution and root development in *Arabidopsis*, Plant Cell 11 (1999) 1217–1226.
[17] A. Sessions, D. Weigel, M.F. Yanofsky, The *Arabidopsis thaliana MERISTEM LAYER 1* promoter specifies epidermal expression in meristems and young primordia, Plant J. 20 (1999) 259–263.
[18] R. Tavares, S. Aubourg, A. Lecharny, M. Kreis, Organization and structural evolution of four multigene families in *Arabidopsis thaliana*: *AtLCAD*, *AtLGT*, *AtMYST* and *AtHD-GL2*, Plant Mol. Biol. 42 (2000) 703–717.
[19] Y.G. Liu, N. Mitsukawa, T. Oosumi, R.F. Whittier, Efficient isolation and mapping of *Arabidopsis thaliana* T-DNA insert junctions by thermal asymmetric interlaced PCR, Plant J. 8 (1995) 457–463.
[20] S.T. Chisholm, S.K. Mahajan, S.A. Whitham, M.L. Yamamoto, J.C. Carrington, Cloning of the *Arabidopsis RTM1* gene, which controls restriction of long-distance movement of tobacco etch virus, Proc. Natl. Acad. Sci. U. S. A. 97 (2000) 489–494.
[21] L.K. Johansen, J.C. Carrington, Silencing on the spot. Induction and suppression of RNA silencing in the Agrobacterium-mediated transient expression system, Plant Physiol. 126 (2001) 930–938.
[22] S.J. Clough, A.F. Bent, Floral dip: a simplified method for *Agrobacterium*-mediated transformation of *Arabidopsis thaliana*, Plant J. 16 (1998) 735–743.
[23] J.W. Wang, L.J. Wang, Y.B. Mao, W.J. Cai, H.W. Xue, X.Y. Chen, Control of root cap formation by MicroRNA-targeted auxin response factors in *Arabidopsis*, Plant Cell 17 (2005) 2204–2216.
[24] N. Mitsuda, M. Seki, K. Shinozaki, M. Ohme-Takagi, The NAC transcription factors NST1 and NST2 of *Arabidopsis* regulate secondary wall thickenings and are required for anther dehiscence, Plant Cell 17 (2005) 2993–3006.
[25] S. Steiner-Lange, U.S. Unte, L. Eckstein, C. Yang, Z.A. Wilson, E. Schmelzer, K. Dekker, H. Saedler, Disruption of *Arabidopsis thaliana MYB26* results in male sterility due to non-dehiscent anthers, Plant J. 34 (2003) 519–528.
[26] C. Yang, Z. Xu, J. Song, K. Conner, G. Vizcay Barrena, Z.A. Wilson, *Arabidopsis MYB26/MALE STERILE35* regulates secondary thickening in the endothecium and is essential for anther dehiscence, Plant Cell 19 (2007) 534–548.
[27] D. Weigel, J.H. Ahn, M.A. Blazquez, J.O. Borevitz, S.K. Christensen, C. Fankhauser, C. Ferrandiz, I. Kardailsky, E.J. Malancharuvil, M.M. Neff, J.T. Nguyen, S. Sato, Z.Y. Wang, Y. Xia, R.A. Dixon, M.J. Harrison, C.J. Lamb, M.F. Yanofsky, J. Chory, Activation tagging in *Arabidopsis*, Plant Physiol. 122 (2000) 1003–1013.
[28] D.H. Jeong, S. An, H.G. Kang, S. Moon, J.J. Han, S. Park, H.S. Lee, K. An, G. An, T-DNA insertional mutagenesis for activation tagging in rice, Plant Physiol. 130 (2002) 1636–1644.
[29] V.B. Busov, R. Meilan, D.W. Pearce, C. Ma, S.B. Rood, S.H. Strauss, Activation tagging of a dominant gibberellin catabolism gene (GA 2-oxidase)

from poplar that regulates tree stature, Plant Physiol. 132 (2003) 1283–1291.

[30] M.A. Ayliffe, M. Pallotta, P. Langridge, A.J. Pryor, A barley activation tagging system, Plant Mol. Biol. 64 (2007) 329–347.

[31] S.Y. Yoo, K. Bomblies, S.K. Yoo, J.W. Yang, M.S. Choi, J.S. Lee, D. Weigel, J.H. Ahn, The 35S promoter used in a selectable marker gene of a plant transformation vector affects the expression of the transgene, Planta 221 (2005) 523–530.

[32] P.M. Sanders, P.Y. Lee, C. Biesgen, J.D. Boone, T.P. Beals, E.W. Weiler, R.B. Goldberg, The *Arabidopsis DELAYED DEHISCENCE1* gene encodes an enzyme in the jasmonic acid synthesis pathway, Plant Cell 12 (2000) 1041–1061.